

IMPROVEMENTS OF NSLS-II X-RAY DIAGNOSTIC BEAMLINES*

W. X. Cheng[#], B. Bacha, B. Kosciuk, D. Padrazo
 NSLS-II, Brookhaven National Laboratory, Upton, NY 11973, USA

Abstract

There are two X-ray diagnostic beamlines (XDB) developed at NSLS-II storage ring to measure emittance, energy spread, and other machine parameters. The first beamline utilizes a soft bending magnet radiation has been in operation since 2014. The tungsten pinhole originally located in the air had corrosion issue. The beamline has been improved by extending the vacuum to the imaging system. The second X-ray pinhole beamline using three-pole wiggler (TPW) radiation has been constructed and commissioned recently. Energy spread is able to be precisely measured due to large dispersion at the source point. A gated camera is equipped with the new beamline to acquire profiles within one turn. Recent operation experience and beam measurements will be presented in this paper.

INTRODUCTION

NSLS-II storage ring was designed to have sub-nm horizontal emittance combining the soft dipoles of double-bending achromatic lattice and damping wigglers. Vertical emittance of 8 pm.rad (diffraction limit of 0.1nm radiation) and lower has been demonstrated. Two X-ray diagnostic beamlines (XDB) have been designed and constructed to precisely measure the transverse emittance and energy spread [1,2].

The first XDB was constructed and commissioned in 2014, using X-ray radiation from the first dipole in the cell #22 (BMA). The pinhole assembled from the tungsten slits experienced corrosion issue and blocked the X-ray radiation. Besides, the X-ray was attenuated while passing through more than 15 meters of air before reaching the scintillator and the imaging system, which limits profile measurement at low current. A reliable emittance measurement was only possible with >20mA stored in the ring. A low vacuum chamber (0.01 – 0.001 torr) was added to extend the beamline vacuum towards the imaging system. This addressed both corrosion and air attenuations issues.

A second XDB was constructed and commissioned in 2017, using the X-ray radiation from the three-pole wiggler (TPW). The TPW has a nominal magnetic field of 1.14 Tesla (compared to the nominal dipole field of 0.4 T). The TPW beamline has more photons which allow profile measurement at much lower current. Additionally, the source point at TPW beamline has a dispersion of ~ 0.17m. The energy spread contribution to the horizontal beam size is comparable, or even larger than the emittance contribution. The layout of the TPW beamline is similar to the BMA beamline. A gated camera [3] imaging system is available for the TPW beamline which

is capable of measuring turn-to-turn profiles.

Figure 1 shows the block diagram of the XDB. A diamond window with thickness of 0.5mm separates the storage ring vacuum and the beamline vacuum which has another 75um thick diamond window at the end. A set of pinholes with various sizes formed by Tungsten slits housed in the box with bellows on both ends. The pinhole assembly box is mounted on a motor stage with X/Y/X'/Y' adjustments. Aluminum bar with different thickness can be inserted to attenuate the X-ray photons. The imaging system formed by a scintillator, a reflection mirror, an objective lens and CCD camera is mounted on an X/Y motor stage. Major parameters of the two XDB are listed in the Table 1.

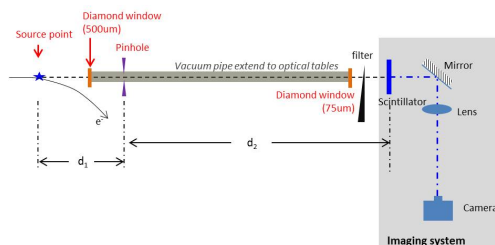


Figure 1: Layout of the NSLS-II storage ring XDB beamline. d_1 is the distance from the source point to pinhole and d_2 is the distance from the pinhole to the scintillator.

Table 1: Parameters of NSLS-II XDB Beamlines

Parameters	BMA	TPW	Note
Source field [T]	0.4*	1.14	*source in the BMA edge
Pinhole size [um]	25	27	Optimized for 15 keV photon
d_1 [m]	3.02	5.3	Source point to pinhole
d_2 [m]	12.98	16.5	Pinhole to scintillator screen
Mx	4.3	3.1	X-ray pinhole magnification
Mv	3	5	Visible image magnification
β_x/β_y [m]	3.7/25	3.8/18.8	Source point beta function
η_x [m]	0	0.17	Dispersion

BMA BEAMLINE UPGRADE

The pinhole assembly was originally in the air, located right after the 0.5mm diamond window (1mm/5mm horizontal/vertical size). After a short period of high current operation (50mA stored beam in 2015), the BMA XDB was not able to see an image. Further investigation revealed that the pinhole had corrosion and was blocked. Figure 2 shows the image of the first slit facing X-ray. The slit surface was polished to optical quality and shining before exposed to X-ray. The black spots in the

*Work supported by DOE contract No: DE-SC0012704
[#]chengwx@bnl.gov

figure were the locations where X-ray hitting the Tungsten slit. The surface had green and white spots which were likely due to ozone generated by X-ray in the air. The nearby diamond window had white/green powder deposited on the window itself and nearby flanges, as seen in the right picture.

Considering the pinhole corrosion in the air and air absorption of the low energy X-ray photons, it was decided to extend the XDB vacuum. The pinhole Tungsten assembly was redesigned to be housed in an Aluminum box, which has bellows on both ends so that the pinhole can be adjusted to align the X-ray radiation. Four different sizes of pinholes can be selected. A vacuum pipe extended towards the optical table where the imaging system is installed, with about $1e-3$ to $1e-2$ torr air pressure. A scroll pump is used to maintain the pressure within range. Vibrations caused by the pump had been investigated with little effect on the nearby storage ring components. At the downstream end of the extension pipe, another $75\mu\text{m}$ thick diamond window is used. There are protection flanges designed with air-fin cooling, to make sure mis-steer beam will not damage the chamber and downstream window assembly.



Figure 2: (left) original in-air pinhole assembly (Tungsten slits) saw corrosion, after a short period of 50mA operation. (right) white/green powders deposited at the diamond window.

After the extended vacuum pipe, X-ray travels in the air for $\sim 20\text{cm}$ before reaching the scintillator. Attenuation of the air is significantly decreased. An Aluminum bar with step-changed thickness can be inserted to filter the low energy photons. A sharp edge Tungsten block is mounted on the filter bar to be used for resolution checking of the imaging system.

The imaging system made up with a scintillator (CaWO_4), Mitutoyo 3x (or 5x) objective lens and a Prosilica GigE CCD camera. Focusing of the visible imaging system was preliminarily adjusted with a test target and fine-tuned with the X-ray beam. The imaging system, as well as the pinhole slits and Al filter bar, are all mounted on motor stages.

TPW BEAMLINER

A second XDB beamline was recently constructed. The new beamline has a similar configuration to the existing BMA XDB, except the new beamline uses X-ray radiation from the TPW. As the TPW has a stronger magnetic field, harder X-ray and more photons are expected. Photon flux from TPW and BMA is compared in Figure 3, where the dash lines are the flux for 0.4T

bending magnet and 1.14T TPW within $10\mu\text{rad} \times 10\mu\text{rad}$ aperture; the solid lines are the flux after the $500\mu\text{m}$ and $75\mu\text{m}$ diamond windows. Without further attenuation from the Al filter, the TPW beamline is expected to have 7 times more photons (up to 20keV) compare to BMA. This allows precise beam size measurement at lower current.

Benefit from the high flux at TPW beamline, it is possible to measure turn to turn profile (or even within a turn, limited by scintillator response time) with a fast gated camera. During the early stage of NSLS-II storage ring operation, lifetime variation along the bunch train was observed [4]. We considered the possible reason was due to fast ion caused beam size change. With the gated camera and fast response scintillator, one can precisely measure the transverse sizes at different parts of the bunch train. Additionally, turn-to-turn profile measurement enabled by the gated camera will be beneficial for beam dynamics studies.

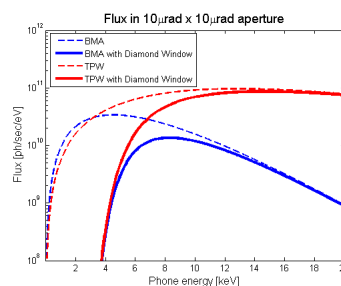


Figure 3: Photon flux comparison of BMA/TPW XDB beamlines. Dashed lines are flux without any filtering while the solid lines are flux after the $500\mu\text{m}$ and $75\mu\text{m}$ diamond windows.

The gated camera setup has the same 5x magnification (Table 1) as the normal CCD setup. Field of view (FoV) is limited due to large magnification. For beam dynamics studies, a wider FoV is desired. The optics can be configured to have a lower magnification lens. A mechanical shutter is installed in the gated camera setup to increase the extinct ratio, especially for narrow gate image acquisitions. The gated camera and shutter can be externally triggered to be synchronized with the storage ring injections or other events.

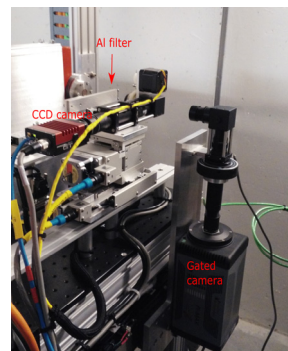


Figure 4: Installed CCD camera and gated camera setups at the TPW XDB beamline end station.

The installed TPW end station is shown in Figure 4, where the CCD camera and gated camera setups are available. Both mounted on X/Y stages that can be aligned to the X-ray beam or fully retracted.

MEASUREMENTS

Resolution of the XDB imaging systems has been optimized in-situ with the X-ray beam. A tungsten bar was inserted to block half of the X-ray radiation. Visible imaging system resolution can be estimated from the edge of the half-blocked image.

Beam emittance can be precisely measured using the pinhole cameras. <3pm.rad vertical has been measured during lattice studies at low current. At high current user operation, the typical vertical emittance is 20-30 pm.rad. Effects of insertion devices gap movement have been observed. Emittance blowup due to top-off injection has been reported at [5]. Even though the centroid motion measured at BPM TbT data damps down quick, typically less than 1ms, the beam size damping took longer time. Similar measurements using gated camera confirm the beam size blows up, while the turn to turn beam centroid is not oscillating.

Less than 8pm.rad vertical emittance was demonstrated during studies at high current, with ~2 hours lifetime (RF voltage 2.25MV). Figure 5 shows the BMA pinhole image at 360mA filled in 1000 bunches. Measured horizontal/vertical emittances are 984.65/7.43 pm.rad respectively, assuming the beta-function at source point of 3.7/25 m, as listed in Table 1.

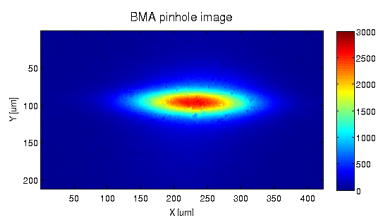


Figure 5: Measured BMA XDB pinhole image at 360mA, horizontal/vertical emittances are 984.65/7.43 pm.rad respectively.

With the second XDB beamline constructed recently, precise energy spread can be measured according to the following equation, as horizontal emittance is known from the 0-dispersion BMA pinhole.

$$\sigma_x^2 = \epsilon_x \beta_x + \left(\eta_x \frac{\sigma_E}{E} \right)^2 \quad (1)$$

Due to its large dispersion and small β_x , TPW pinhole image is sensitive to energy spread variation. Early studies [6] have shown energy spread increase when single bunch current is higher than ~0.5mA (bare lattice with damping wigglers gap open), measured at the visible diagnostic beamline. A similar measurement of energy spread vs. single bunch current has been carried out recently using TPW pinhole beamline with much improve resolution, the result is available in Figure 6. The

calculated energy spread starts increasing at pretty low single bunch current and has step changes at ~0.7mA, 1.6mA etc. The step changes agree with the sidebands transient noticed on the synchrotron sideband spectra [6].

To measure turn to turn (or within one turn) profile, the scintillator has to have short decay time. Two types of the scintillator (YAG:Ce and LSO:Ce) with fast decay time and high photon yield [7,8] have been tested for the gated camera setup at TPW diagnostic beamline. Images with different gate delays have been acquired during normal operation (with 1000 bunches filled) and short bunch train fills (typically 20 bunches). LSO scintillator has fast decay time measured, although both screens can be used to measure turn-to-turn transverse profiles. The decay time of LSO screen we have is about 300ns, including the afterglow.

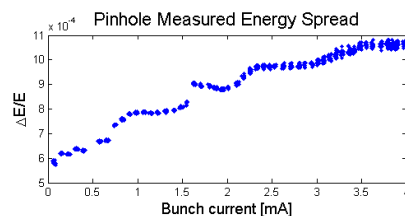


Figure 6: Energy spread measured at different single bunch current, with bare lattice and RF voltage of 2.25MV.

To verify the bunch size increase due to fast ion trapping, gated camera images along the bunch train have been captured. After a recent vacuum work to remove one of the insertion devices, the machine started up had large vertical emittance. Gated camera measurement along the bunch train clearly show vertical size increases of tail bunches. Figure 7 shows the gated camera measured sizes. The gate width was fixed at 100ns while increasing the delay in 100ns steps. The vertical size increases phenomenon was not obvious after hours of high current conditioning. Note vertical emittance was relatively large while taking the gated camera images, even after vacuum conditioning. It will be interesting to repeat the same measurement at < 8pm.rad vertical emittance with high current stored in the ring.

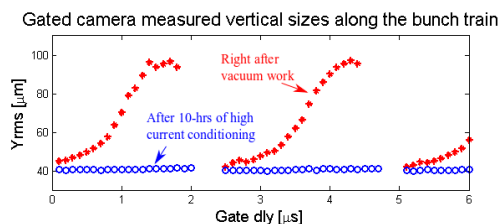


Figure 7: Gated camera measure vertical sizes along the bunch train, with 375mA stored in 1000 bunches.

SUMMARY

The BMA pinhole beamline has been improved to address the corrosion and air attenuation issues. A second TPW diagnostic beamline has been recently constructed and enables the possibility to measure beam sizes within a

turn. With the two diagnostic beamlines, storage ring emittance, energy spread, and other machine parameters can be studied with good precision.

The author thanks Om Singh for his support of the improvement work and construction of TPW beamline.

REFERENCES

- [1] I. Pinayev *et al.*, “Preliminary Design of Pinhole Camera for NSLS-II Project”, in *Proc. 23rd Particle Accelerator Conf. (PAC’09)*, Vancouver, Canada, May 2009, paper TH5RFP015, pp. 3473-3475.
- [2] P. Ilinski, “NSLS-II X-ray Diagnostics Development”, in *Proc. Particle Accelerator Conf. (PAC’11)*, New York, NY, USA, Mar.-Apr. 2011, paper MOP199, pp. 468-470.
- [3] Princeton Instruments, <https://www.princetoninstruments.com/products/PI-MAX4-emICCD/>.
- [4] W. Cheng, Y. Li, B. Podobedov, “Experimental evidence of ion-induced instabilities in the NSLS-II storage ring”, *Nucl. Instr. Meth. A*, vol. 861, pp. 38–45, 2017.
- [5] W. X. Cheng *et al.*, “Beam Stability During Top Off Operation at NSLS-II”, in *Proc. North American Particle Accelerator Conf. (NA-PAC’16)*, Chicago, IL, USA, Oct. 2016, paper TUPOA71, pp. 425-427, <https://doi.org/10.18429/JACoW-NAPAC2016-TUPOA71>
- [6] W. X. Cheng *et al.*, “Experimental Study of Single Bunch Instabilities at NSLS-II Storage Ring”, in *Proc. 7th Int. Particle Accelerator Conf. (IPAC’16)*, Busan, Korea, May 2016, paper TUPOR033, pp. 1738-1740, DOI:10.18429/JACoW-IPAC2016-TUPOR033
- [7] <http://scintillator.lbl.gov/>
- [8] MTI Corporation, <http://www.mtixtl.com/>.